Performance of differential phase shift keying maritime laser communication over log-normal distribution turbulence channel*

QIAO Yuan-zhe (乔元哲)[1,2†], **LU Ze-hui** (陆泽辉)[2†], **YAN Bao-luo** (闫宝罗)[2], **LI Chang-jin** (李昌瑾)[2], **ZHANG Hao** (张昊)[2], **LIN Wei** (林炜)[2,3], **LIU Hai-feng** (刘海锋)[2,3], **and LIU Bo** (刘波)[2,3]**

1. Beijing Institute of Remote Sensing Equipment, Beijing 100039, China

2. Tianjin Key Laboratory of Optoelectronic Sensor and Sensing Network Technology, Institute of Modern Optics, Nankai University, Tianjin 300350, China

3. Southern Marine Science and Engineering Guangdong Laboratory, Zhuhai 519000, China

(Received 9 December 2019; Revised 31 December 2019)

Laser communication is essential part of maritime-terrestrial-air intelligent communication/sensor network. Among them, different modulation formats would play a unique role in specific applications. Based on Rytov theory, we discussed system performance of the maritime laser communication with repeated coding technology in several modulation schemes. The closed-form expression of average bit error rate (*BER*) from weak to moderate atmospheric turbulence described by log-normal distribution is given. Differential phase shift keying (DPSK) modulation, as a potential solution for future maritime laser communication, has attracted a lot of attention. We analyzed the effects of atmospheric turbulence parameters (visibility, refractive index structure coefficient, non-Kolmogorov spectral power-law exponent, turbulence inner scale) and DPSK system parameters (receiver aperture diameter, repeat time) on average *BER* in detail. Compared with the aperture-averaging effects, the system *BER* can be well suppressed through increasing repeat time. This work is anticipated to provide a theoretical reference for maritime laser communication systems.

Document code: A **Article ID:** 1673-1905(2021)02-0090-6

DOI https://doi.org/10.1007/s11801-021-9211-9

Taking the advantages of their large bandwidth, high capacity, ease of deployment, unlicensed spectrum, free space optics (FSO) have been widely applied to the fields of satellite-ground, air-ground, island-shore, underwater laser communication, etc. However, the low transmission rate of beam in free space greatly limits the service range of the FSO. Atmospheric turbulence would bring many negative effects, such as beam wandering, fluctuating angle of arrival, beam expansion, spot distortion and intensity scintillation, which severely limit the distance and communication speed. Turbulence channel models help us understand the negative effects of turbulence on communications system. The Gamma-Gamma channel model fits for week to strong turbulence, while the log-normal (LN) channel is modelled for week to moderate turbulence, and Negative exponential channel model is suitable for long-distance condition[1]. Moreover, some solutions with excellent turbulence suppression ability have been applied in practical engineering, such as multiple-input-multiple-output technique[2], amplify-and-forward relaying technique[3], combined radio frequency (RF)/FSO network[4], adaptive optical pre-compensation technique[5]. In addition, some anti-fading coding and modulation schemes are also effective, such as time diversity realized by repeated coding[6], robust binary phase shift keying (BPSK)[7].

There are a surge of interest in maritime wireless optical communication for developing maritime-terrestrial-air information fusion network[8]. Benefiting from the ease of deployment, FSO is a promising solution for connected islands. European Space Agency (ESA) conducted the inter-island optical communication experiment along a 150 km path at an altitude of 2 400 m over the Canarian archipelago in 1995[9]. However, a challenging problem is that complex atmospheric turbulence limits communication distance. In 2009, Juan C. Juarez et al[10] carried out ship-to-shore 2.5 Gbit/s wireless communication over 22 km maritime environment with the help of adaptive optics system, which provides ~1° tracking accuracy. More

* This work has been supported by the National Key R&D Program of China (No.2018YFB1802302), the National Natural Science Foundation of China (Nos.11774181, 61727815, 11274182, 11904180, 11804250 and 1190426), the Science and Technology Support Project of Tianjin (No.16YFZCSF00400), the Natural Science Foundation of Tianjin (No.19JCYBJC16700), and the Tianjin Development Program for Innovation and Entrepreneurship.

† These authors contributed equally to this work.

** E-mail: liubo@nankai.edu.cn

over, FSO with RF assisted is another effective solution. Mark Gregory et al[11] investigated the communication data in a 14 km hybrid RF/FSO maritime channel to provide effective channel estimates between May and Dec 2010. Also, some theoretical results deepened our understanding of FSO in maritime environment. In 2016, Hyeong-Ji Kim et al[12] used Gamma-Gamma distribution to study relay-based maritime visible light communication. They found that maximal ratio-combining scheme gives a superior bit error rate (*BER*) performance. Ming Li et al[13] evaluated the coherent FSO system employing quadrature array phase-shift keying (QPSK) modulation over the maritime and terrestrial atmospheric links. Their result indicated that the maritime FSO system possess the higher *BER* compared with the terrestrial FSO under the same turbulence strength. Maritime optical communications should be affected by seawater, but there is no need to consider temperature, salinity and depth like underwater optical communication systems[14]. We need a suitable and accurate theoretical model to describe the maritime turbulence. Cheng et al[15] shows that weak non-Kolmogorov maritime atmospheric turbulence channel can be characterized by LN distribution. Moreover, based on the measured data in the ship-to-land communication at the Baltic Sea, H. Henniger et al[16] confirm the validity of the LN statistical model in describing maritime turbulence.

Most of the current theoretical studies related to maritime FSO channel are based on intensity modulation/direct detection methods. We need to fully understand the performance of various modulation schemes. With high robustness and anti-fading ability, DPSK format has been used for long-distance scenes[17]. In this letter, the influence of turbulence parameters and system parameters on the average *BER* are investigated in detail, which expected to provide important reference for the realization of optical communication in maritime environment.

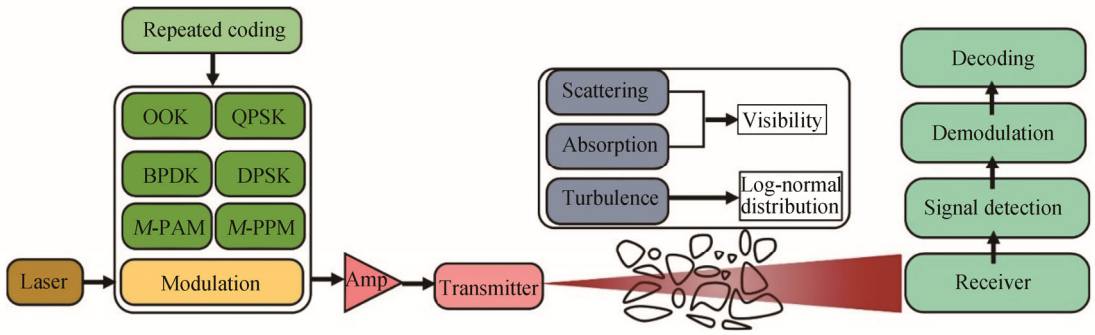

Fig.1 Block diagram of maritime laser communication system based on repeated coding with various modulation

Fig.1 shows a simplified block diagram of maritime laser communication system. Signals are coded by repeated coding technology to implement time diversity, and then modulated by on-off keying (OOK), BPSK, QPSK, DPSK, *M*-pulse amplitude modulation (*M*-PAM), *M*-pulse position modulation (*M*-PPM). Next, the optical signal can achieve enough gain through the fiber amplifier and transmit to the free space through the transmit antenna. Considering the influence of atmospheric turbulence, we introduce atmospheric visibility V to describe the scattering and absorption, and LN distribution to describe the effects of turbulence-induced intensity scintillation, etc. The receiver uses a larger aperture antenna to achieve efficient spatial light-fiber coupling through aperture-averaging effects. After pre-amplification, opto-electrical conversion and a series of digital signal processing (DSP), signal can be recoverd in the receiver end.

Atmospheric losses can be described by the Beer-Lambert's law[18]:

$$I_l=\exp(-\beta_l L), \tag{1}$$

$$\beta_l=10\lg\left(\frac{0.114\,78\lambda+3.867}{V}\right)(\text{dB/km}), \tag{2}$$

where β_l is attenuation coefficient caused by atmospheric absorption for wavelength located bewteen 0.69 μm and 1.55 μm. L is the communication distance, V is atmospheric visibility in km, and λ is wavelength in μm.

Considering the beams divergence during propagation, the receiver beam parameters Θ, Λ and $\overline{\Theta}$ at distance L can be expressed by curvature paratemer Θ_0 and Fresnel ratio at the transmitter Λ_0:

$$\Theta=\Theta_0/(\Theta_0^2+\Lambda_0^2), \tag{3}$$

$$\Lambda=\Lambda_0/(\Theta_0^2+\Lambda_0^2), \tag{4}$$

$$\overline{\Theta}=1-\Theta, \tag{5}$$

$$\Theta_0=1-L/F, \tag{6}$$

$$\Lambda_0=2L/(k\omega_0^2), \tag{7}$$

where F, k and ω_0 are the phase front radius of curvature, wave vector and waist width of beams at transmitter, respectively.

The propagation process can be simplified to the following process. The Gaussian beam with different modulation schemes passes through the weak non-Kolmogorov maritime atmospheric turbulence channel and superimposes additive white Gaussian noise (AWGN). The received electrical signal is given by:

$$y=Ix+n, \tag{8}$$

where y is the received signal, x is the modulated signal, n is white Gaussian noise. $I=I_aI_l$ is the instantaneous fading caused by atmospheric turbulence, which including path losses I_l and attenuation caused by atmospheric

turbulence I_a.

Without atmospheric turbulence, conditional *BER* can be expressed as a function of signal-to-noise ratio (*SNR*) in several common modulation schemes[19-21]:

$$BER'_{\text{RZ-OOK}}(I)=\frac{1}{2}erfc(\frac{1}{2}\sqrt{SNRI}=Q(\sqrt{SNR/2I}), \quad (9)$$

$$BER'_{\text{BPSK}}(I)=\frac{1}{2}erfc(\sqrt{SNRI}=Q(\sqrt{2SNRI}), \quad (10)$$

$$BER'_{\text{QPSK}}(I)=erfc(\sqrt{SNRI}=2Q(\sqrt{2SNRI}), \quad (11)$$

$$BER'_{\text{DPSK}}(I)=\frac{1}{2}erfc(\sqrt{SNR/2I}=Q(\sqrt{SNRI}) \quad (12)$$

$$BER'_{\text{M-PPM}}(I)=\frac{1}{2}erfc(\frac{\sqrt{SNR\frac{M}{2}\log_2(M)}}{2\sqrt{2}}I)=Q(\frac{\sqrt{SNR\frac{M}{2}\log_2(M)}}{2}I), \quad (13)$$

$$BER'_{\text{M-PPM}}(I)=\frac{1}{2}erfc(\frac{\sqrt{SNR\log_2(M)}}{2\sqrt{2}(M-1)}I)=Q(\frac{\sqrt{SNR\log_2(M)}}{2(M-1)}I), \quad (14)$$

where $Q(x)$ is Gaussian-Q function:

$$Q(x)=1/\sqrt{2\pi}\int_x^{+\infty}\exp(-t^2/2)\,dt=erfc(x/\sqrt{2})/2, \quad (15)$$

and M represents the level of pulse position/amplitudes code.

Further, to consider the scintillation effects, LN probability density function (PDF) is introduced $\sigma^2_{\ln I}$ to describe weak to moderate atmospheric turbulence[1]:

$$f(I)=\frac{1}{I\sqrt{2\pi\sigma^2_{\ln I}}}\exp\left\{\frac{-\left[\ln(I/I_l)+0.5\sigma^2_{\ln I}\right]^2}{2\sigma^2_{\ln I}}\right\}, \quad (16)$$

where log-intensity variance $\sigma^2_{\ln I}$ can be expressed by intensity scintillation index $\sigma^2_{\ln I}=A\ln(\sigma_I^2+1)$. Intensity scintillation index σ_I^2 is given by[15]:

$$\sigma_I^2=4\pi^2k^2LA(\alpha)C_n^2\kappa_m^{2-\alpha}\times\left\{\Gamma\left(\frac{2-\alpha}{2}\right)\mathrm{Re}\left[{}_2F_1\left(\frac{2-\alpha}{2},\frac{1}{2};\frac{3}{2};-\Lambda Q_m\right)-{}_2F_1\left(\frac{2-\alpha}{2},1;2;\frac{2}{3}(\mathrm{i}Q_m\overline{\Theta}-\Lambda Q_m)-\mathrm{i}Q_m\right)\right]-0.061\Gamma\left(\frac{3-\alpha}{2}\right)\mathrm{Re}\left[{}_2F_1\left(\frac{3-\alpha}{2},\frac{1}{2};\frac{3}{2};-\Lambda Q_m\right)-{}_2F_1\left(\frac{3-\alpha}{2},1;2;\frac{2}{3}(\mathrm{i}Q_m\overline{\Theta}-\Lambda Q_m)-\mathrm{i}Q_m\right)\right]+2.836\Gamma\left(\frac{10-3\alpha}{4}\right)\mathrm{Re}\left[{}_2F_1\left(\frac{3-\alpha}{2},\frac{1}{2};\frac{3}{2};-\Lambda Q_m\right)-{}_2F_1\left(\frac{10-3\alpha}{4},1;2;\frac{2}{3}(\mathrm{i}Q_m\overline{\Theta}-\Lambda Q_m)-\mathrm{i}Q_m\right)\right\}, \quad (17)$$

where $\kappa_m=\{A(\alpha)\Gamma[(5-\alpha)/2]2\pi/3\}^{1/(\alpha-5)}/l_0$, $Q_m=\kappa_m^2L/k$, $\Gamma(x)$ is gamma function, and ${}_2F_1(x)$ is generalized hypergeometric function, C_n^2 is refractive index structure coefficient in $\mathrm{m}^{3-\alpha}$, and $A(\alpha)$ is a constant that maintains consistency bewteen the refractive index structure function and its power spectrum, which is defined as

$$A(\alpha)=\Gamma(\alpha-1)\cos(\alpha\pi/2)/4\pi^2. \quad (18)$$

For optical communication over LN distribution channel, aperture-averaging factor is defined as:

$$A=\frac{16}{\pi}\int_0^1 x\exp\left[\frac{-D_s^2x^2}{\rho_T^2}\left(2+\frac{\rho_T^2}{\omega_0^2\Lambda_0^2}-\frac{\rho_T^2\varphi^2}{\omega_\zeta^2}\right)\right]\times\left[\arccos(x)-x\sqrt{(1-x^2)}\right]dx, \quad (19)$$

where $\rho_T=\left[1.46k^2L\int_0^1 C_n^2(1-\zeta)^{5/3}\,d\zeta\right]^{-3/5}$, $\varphi=\Theta_0/\Lambda_0-\Lambda_0\omega_0^2/\rho_T$ and $\omega_\zeta=\omega_0\sqrt{(\Theta_0^2+\Lambda_0^2)}$.

Take atmospheric turbulence and diversity effects of repeated coding into account, average *BER* is given by[6]

$$BER=\int_0^\infty BER'(I)\cdot f(I)\times\frac{1}{(L_n-1)!}\left(\frac{I}{I_l}\right)^{L_n-1}dI. \quad (20)$$

In order to derive the closed expression of the system average *BER*, let $x_i=[\ln(I/I_l)+\sigma^2_{\ln I}/2]/(2\sigma^2_{\ln I})^{1/2}$, then get $I(x_i)=I_l\exp(\sqrt{2}\sigma_{\ln I}x_i-\sigma^2_{\ln I}/2)$ and $dI=I\sqrt{2}\sigma_{\ln I}\,dx_i$. By using Gauss-Hermite quadrature integration approximation $\omega_i=(2^{n-1}n!\sqrt{\pi})/(n^2H_{n-1}(x_i)^2)$, Eq.(20) can be efficiently approximated as

$$BER=\int_0^\infty 1/(\sqrt{2\pi\sigma^2_{\ln I}})\cdot e^{-x^2}\cdot BER'\cdot(1/(L_n-1)!)\cdot(I/I_l)^{L_n-1}\cdot I\sqrt{2\sigma^2_{\ln I}}\,dx=(2^{n-1}\cdot n!)/n^2\cdot(1/(L_n-1)!)\cdot\sum_1^n(1/H_{n-1}(x_i)^2)\cdot c_1Q(\sqrt{SNR\cdot c_2}\cdot I_l\cdot e^{\sqrt{2}\sigma_{\ln I}-\sigma^2_{\ln I}/2})\cdot e^{(\sqrt{2}\sigma_{\ln I}-\sigma^2_{\ln I}/2)(L_n-1)}, \quad (21)$$

where x_i are the roots of the Hermite polynomial $H_n(x_i)$. As shown in Tab.1, c_1 and c_2 are characteristic constants for various modulation techniques.

Tab.1 c_1 and c_2 for various modulation techniques

Modulation	c_1	c_2	Modulation	c_1	c_2	Modulation	c_1	c_2
RZ-OOK	1	1/2	QPSK	2	2	*M*-PPM	1	$\frac{M}{8}\log_2(M)$
BPSK	1	2	DPSK	1	1	*M*-PAM	1	$\frac{\log_2(M)}{4(M-1)^2}$

According to the above analysis, we can clearly understand that the system average *BER* should be related to the modulation formats, system parameters, and turbulence parameters. Next, we define some global parameters to characterize the system performance under weak non-Kolmogorov maritime atmospheric environments as shown in Tab.2.

The average *BER* as a function of *SNR* for various modulation techniques over weak non-Kolmogorov maritime atmospheric turbulence channel are shown in Fig.2. For the same system *BER*, *M*-PPM requires the lowest *SNR*

compared with other modulation schemes, in other words, it possess minimum transmit power demand. As M increases, the number of time slots increases, and the energy efficiency of M-PPM improves, so its average transmit power will be further reduced. However, this could lead to a lot of bandwidth waste[22], which is an inherent disadvantage of the PPM modulation format. Instead, M-PAM has extremely high bandwidth effciency[23] but lowest energy efficiency at the same time, just as its *BER* curve is located at the highest position. And that is why PPM is suitable for long-distance, high-fading communication, such as maritime[6], underwater[24], deep space FSO[22], while PAM is more applicable to short-distance and high-capacity demand, such as 5G wireless networks[25]. Taking the advantages of their simple system architecture and mature technology, OOK format have been widely applied to FSO, but one of the inevitable issues required to be resolved is that the receiver needs a dynamic threshold detector to track the fluctuating signal due to its low noise immunity. As shown in Fig.2, PSK curves are located in the middle position, which means that PSK can make a compromise between spectrum efficiency and energy utilization. Moreover, BPSK possess relatively power robustness and high spectral efficiency, which has been applied to FSO between two 142 km Canary islands[26]. Furthermore, DPSK can solve the phase ambiguity phenomenon of BPSK. In the maritime communication system, DPSK could be a promising way besides PPM modulation.

Tab.2 Parameters used in numerical calculation

Parameter	Symbol	Value
Wavelength (μm)	λ	1.55
Waist width (m)	ω_0	0.01
Visibility (km)	V	1
Refractive index structure coefficient ($m^{3-\alpha}$)	C_n^2	1×10^{-14}
Receiver aperture diameter (m)	D_s	0.02
Signal to noise ratio (dB)	*SNR*	20
Repeat time	L_n	5
Turbulence inner scale (mm)	l_0	7
Non-Kolmogorov spectral power-law exponent	α	3.3
The phase front radius of curvature (m)	F	1 000

Fig.3. reveals the effect of turbulence and system parameters on average *BER* with repeated coding technology. In Fig. 3(a), the system simulation parameters are set to λ=1.55 μm, ω_0=0.01 m, V=1 000 m, $C_n^2=1\times10^{-14}$ $m^{3-\alpha}$, *SNR*=20 dB, L_n=5, l_0=7 mm, α=3.3 and F=1 000 m. The communication distance can be extended by 239 m through increasing the receiver aperture diameter D_s from 3 cm to 6 cm under the determined *BER* (10^{-8}). Moreover, we noticed that as the distance increases, the gain from aperture-averaging effects would be weakened due to the beam divergence. In Fig.3(b), the system simulation parameters are set to λ=1.55 μm, ω_0=0.01 m, V=1 000 m, $C_n^2=1\times10^{-14}$ $m^{3-\alpha}$, D_s=0.02 m, *SNR*=20 dB, l_0=7 mm, α=3.3 and F=1 000 m. The system average *BER* is reduced by 31.1 dB with the increase of the diversity repeat time L_n from 1 to 5 at 2000 m, which illustrates that the error probability in the decoding process can be effectively reduced by repeated coding schemes, but it sacrifices communication speed. Considering the absorption effect of the atmosphere, the visibility V of 1 km represents dense fog, while V of 10 km corresponds to thin fog[27]. In Fig.3(c), the system simulation parameters are set to λ=1.55 μm, ω_0=0.01 m, $C_n^2=1\times10^{-14}$ $m^{3-\alpha}$, D_s=0.02 m, *SNR*=20 dB, L_n=5, l_0=7 mm, α=3.3 and F=1 000 m. Comparing the two *BER* curves with V=1 km and V=10 km at 2 000 m, we found that harsh weather caused the system *BER* to degrade by 40.4 dB. Turbulence can be defined by refractive index structure coefficient C_n^2 as weak turbulence (10^{-16} $m^{3-\alpha}$), moderate turbulence (10^{-14} $m^{3-\alpha}$) and strong turbulence (10^{-13} $m^{3-\alpha}$)[1]. In Fig.3(d), we study the influence of C_n^2 on system performance. The system simulation parameters are set to λ=1.55 μm, ω_0=0.01 m, V=1 000 m, D_s=0.02 m, *SNR*=20 dB, L_n=5, l_0=7 mm, α=3.3 and F=1 000 m. Under the same *BER* (10^{-8}), the communication distance was extended by 567 m after the turbulence intensity changed from moderate to weak condition (10^{-14}—10^{-15} $m^{3-\alpha}$).

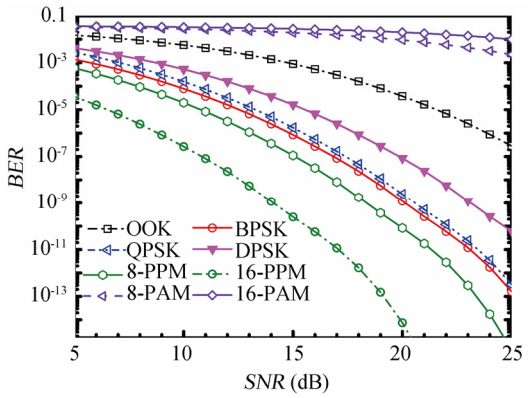

Fig.2 Average *BER* vs. *SNR* for various modulation formats in weak non-Kolmogorov maritime atmospheric environment

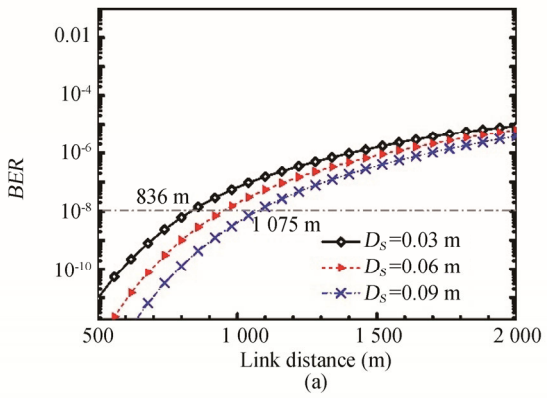

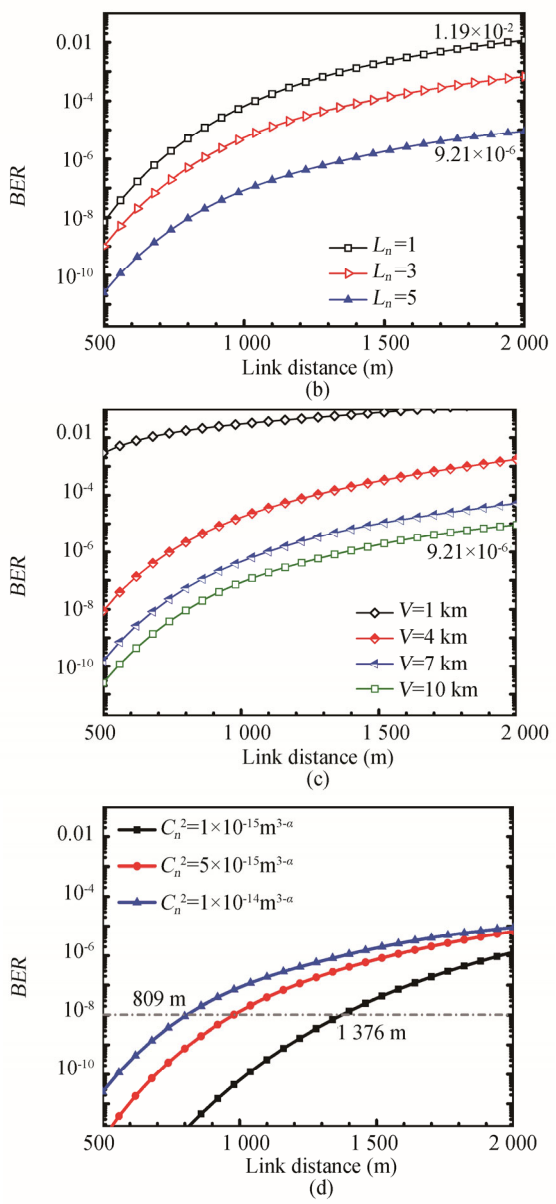

Fig.3 Average *BER* vs. link distance for various values of (a) receiver aperture diameter, (b) repeat time, (c) visibility and (d) refractive index structure coefficient in weak non-Kolmogorov maritime atmospheric environment

Atmospheric turbulence parameters (e.g. turbulence inner scale l_0, refractive index structure coefficient C_n^2 and non-Kolmogorov spectral power-law exponent α) can severely affect the intensity scintillation index σ_I^2 and further interfere with the beam. Thus, optimized design of system parameters (e.g. receiver aperture diameter D_s and repeat time L_n.) would improve the robustness of the system. We give the 3D relationship of the influence of these variables on the system *BER* based on Eq.(21). In Fig.4(a), the system *BER* increases if α, V decreases or C_n^2, l_0 increases. Further, by comparing the changes in the curvature of the 3D surface, we can concluded that (1) the influence on *BER* from high to low are V, C_n^2, α and l_0 respectively; (2) as the transmission distance increases, the adverse effect of atmospheric turbulence on *BER* becomes more significant. Here, we mainly considered two mitigation schemes, one is to enhence repeat time L_n and the other is to make full use of the aperture-averaging effects through increasing D_s. As shown in Fig.4(b), the above solutions can both suppress *BER* degradation. In particular, the increasing L_n can more quickly reduce the *BER* compared with D_s based on the evolution of the color bar, which indicated that repeated coding technology would be an effective solution to alleviate oceanic turbulence.

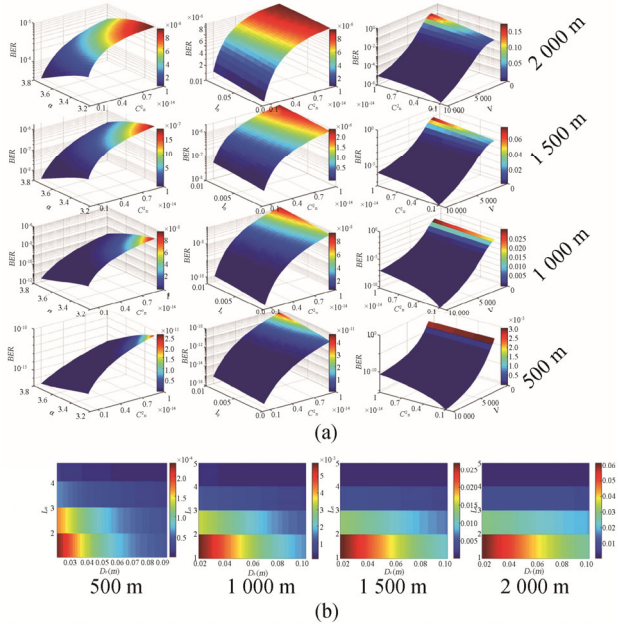

Fig.4 (a) A comparison of turbulent parameters: the relationship of *BER*-α-C_n^2, *BER*-l_0-C_n^2 and *BER*-C_n^2-V; (b) A comparison of system parameters: the relationship of *BER*-D_s-L_n in different transverse planes

In the practical FSO system design, the weak signal detection can be realized through optical amplification. Turbulent channel is a vital factor that must be considered in system power margin. This work provides the relationship between system performance and certain parameters. Based on actual channel and system conditions, we can give approximate estimates, which helps us better design the transceiver system. It should be noted that more accurate theoretical estimates need to further refine the system parameters, such as the gain of the fiber amplifier, noise figure, spatial light-fiber coupling efficiency, tracking accuracy, etc.

In conclusion, based on Rytov theory and generalized turbulent refractive index spectrum, we derived closed-form system *BER* expressions for several modulation formats beam propagating through weak non-Kolmogorov maritime atmospheric environments. It turns out that average transmit power and spectral efficiency of PPM is lowest, conversely, PAM have the highest average transmit power and spectral efficiency, which can be used in

long-distance and high-capacity required systems, respectively. DPSK modulation can balance the advantages of both, so it has more potential applications. In DPSK maritime FSO, the average *BER* reduces with the increment of C_n^2, l_0 and the decrease of α, V. Small V is more likely to induce distortion. Moreover, as distance increases, turbulence would cause greater *BER* deterioration due to cumulative effects. Compared with the aperture-averaging effects, the repeated coding technique is a more promising solution cause it only needs to code a few times and then can largely restore the system performance. The simulation results presented in this work are expected to provide important reference for the design and optimization of maritime optical communication systems.

References

[1] K. Anbarasi, C. Hemanth and R. Sangeetha, Optics & Laser Technology **97**, 161 (2017).

[2] B. B. Yousif and E. E. Elsayed, IEEE Access **7**, 84401 (2019).

[3] X. Huang, X. Xie, J. Song, T. Duan, H. Hu, X. Xu and Y. Su, IEEE Photonics Journal **10**, 7905411 (2018).

[4] H. A. El-Malek, A. M. Salhab, S. A. Zummo and M.-S. Alouini, Journal of Lightwave Technology **35**, 1490 (2017).

[5] Brady, R. Berlich, N. Leonhard, T. Kopf, P. Böttner, R. Eberhardt and C. Reinlein, Optics Letters **42**, 2679 (2017).

[6] D. Tse and P. Viswanath, Fundamentals of Wireless Communication, Cambridge University Press, (2005).

[7] J. Zhao, S.-h. Zhao, W.-h. Zhao, Y.-j. Li, Y. Liu and X. Li, Optics Communications **359**, 189 (2016).

[8] H. Wehna, R. Yates, P. Valin, A. Guitouni, É. Bossé, A. Dlugan and H. Zwicka, A distributed Information Fusion Testbed for Coastal Surveillance, 10th International Conference on Information Fusion, 1 (2007).

[9] Comeron, J. A. Rubio, A. M. Belmonte, E. Garcia, T. Prud'homme, Z. Sodnik and C. Connor, Propagation Experiments in the Near Infrared along a 150-km Path and from Stars in the Canarian Archipelago, Eighth International Symposium on Atmospheric and Ocean Optics: Atmospheric Physics (International Society for Optics and Photonics), 78 (2002).

[10] J. C. Juarez, J. E. Sluz, C. Nelson, M. B. Airola, M. J. Fitch, D. W. Young, D. Terry, F. M. Davidson, J. R. Rottier and R. M. Sova, Free-Space Optical Channel Characterization in the Maritime Environment, Atmospheric Propagation VII (International Society for Optics and Photonics), 76850H (2010).

[11] M. Gregory and S. Badri-Hoeher, Characterization of Maritime RF/FSO Channel, International Conference on Space Optical Systems and Applications, 21 (2011).

[12] H.-J. Kim, S. V. Tiwari and Y.-H. Chung, Chinese Optics Letters **14**, 050607 (2016).

[13] M. Li and M. Cvijetic, Applied Optics **54**, 1453 (2015).

[14] Y. Weng, Y. Guo, O. Alkhazragi, T. K. Ng, J.-H. Guo and B. S. Ooi, Journal of Lightwave Technology **37**, 5083 (2019).

[15] M. Cheng, L. Guo and Y. Zhang, Optics Express **23**, 32606 (2015).

[16] H. Henniger, B. Epple and H. Haan, Maritime Mobile Optical-Propagation Channel Measurements, IEEE International Conference on Communications, 1 (2010).

[17] B. Yan, H. Liu, B. Liu, J. Liu, H, Zhang, C. Yang, Z. Hu and X. Li, IEEE Photonics Journal **11**, 1 (2019).

[18] M. C. Al Naboulsi, H. Sizun and F. de Fornel, Optical Engineering **43**, 319 (2004).

[19] S. M. Navidpour, M. Uysal and M. Kavehrad, IEEE Transactions on Wireless Communications **6**, 2813 (2007).

[20] T. Y. Elganimi, Studying the BER Performance, Power- and Bandwidth-Efficiency for FSO Communication Systems under Various Modulation Schemes, IEEE Jordan Conference on Applied Electrical Engineering and Computing Technologies, 1 (2013).

[21] N. Mehnaz and M. Islam, Performance Analysis of a Coherent Free Space Optical System with Different Modulation Schemes, IEEE International Conference on Telecommunications and Photonics, 222 (2017).

[22] G. Xu, Optics express **27**, 24610 (2019).

[23] K. Zhong, X. Zhou, T. Gui, L. Tao, Y. Gao, W. Chen, J. Man, L. Zeng, A. P. T. Lau and C. Lu, Optics Express **23**, 1176 (2015).

[24] S. Hu, L. Mi,T. Zhou and W. Chen, Optics Express **26**, 21685 (2018).

[25] Z. Zhao, Z. Zhang, J. Tan, Y. Liu and J. Liu, IEEE Photonics Journal **10**, 1 (2018).

[26] R. Lange, B. Smutny, B. Wandernoth, R. Czichy and D. Giggenbach, 142 km, 5.625 Gbps Free-Space Optical Link Based on Homodyne BPSK Modulation, Free-Space Laser Communication Technologies XVIII (International Society for Optics and Photonics), 61050A (2006).

[27] Viswanath, V. K. Jain and S. Kar, Optical and Quantum Electronics **48**, 435 (2016).